Mechanics & Industry **17**, 612 (2016)

DOI: 10.1051/meca/2016009
www.mechanics-industry.org

Mechanics & Industry

TiO_2-water nanofluid within a tilted triangular enclosure including a square heater: optimum heat transfer

Karim Ragui[1], Abdelkader Boutra[1,2,a], Youb Khaled Benkahla[1], Nabila Labsi[1] and M'barek Feddaoui[3]

[1] University of Science and Technology Houari Boumediene, BP 32 El Alia, 16111 Algiers, Algeria
[2] Preparatory School of Science and Technology, EPSTA, Algiers, Algeria
[3] Université Ibnou Zohr, BP 1136-80000, ENSA-Agadir, Morocco

Received 19 October 2015, Accepted 27 January 2016

Abstract – Into this paper, natural convection of TiO_2-water nanofluid is numerically investigated around a square isothermal heater, found into a two-dimensional cold enclosure of an isosceles triangle form. To do so, a computer code based on the finite volume method and the velocity-pressure correction approach, namely SIMPLER, is used. This code has been validated for cases of a base fluid and a Nanofluid, after comparison between the obtained results and the numerical (or experimental) ones already available in the literature. To make clear the effect of main parameters such the Rayleigh number, the solid volume fraction as well as the cavity' inclination angle, the convection phenomenon is reported by means of Streamlines and isotherm plots; with a special attention to the Nusselt number evolution. The results show that the mean Nusselt number is an increasing function of the Rayleigh number and the solid volume fraction, whereas the inclination angle of the cavity has no significant effect on heat transfer. Then, useful correlations which predicting the latter as a function of the solid volume fraction for various Rayleigh values are proposed, which predicts within ±0.4% the numerical results.

Key words: Natural convection / isosceles triangular enclosure / TiO_2-water nanofluid / square heat source / finite volume method

1 Introduction

Heat convection of nano fluids, which are a mixture of nanoparticles in a base fluid such water and oil, has been recently an active field of research since they are used to improve heat transfer. Compared to other techniques for enhancing heat transfer in practical applications, nanofluids have the advantage of behaving like pure fluids because of the nanometric size of introduced solid particles. Thus, it can be used as heat transfer fluids for various applications, such in advanced nuclear systems or micro/mini channel heat sinks, electronic equipment as power transistors, printed wiring boards and chip packages mounted on computer mother boards.

To reveal the effects of such added nanoparticles on the heat transfer, some papers dealing with natural convection of nanofluids into differentially heated enclosures were very helpful [1–4]. A review of the literature indicates that most researches [5–8] were achieved using a square configuration whilst a little attention has been devoted to the convection phenomenon within complex configurations such triangular ones [9–11].

Elif [12] investigated natural convection heat transfer of water-based nanofluids within an inclined square enclosure having a left heat source, with a constant heat flux mounted at its center, and a right cold wall, the remaining walls were maintained adiabatic. The predictions were performed using the polynomial differential quadrature method by taking into account the variation of the inclination angle (from 0° to 90°), the solid volume fractions (from 0% to 20%), the heater' source length (0.25, 0.50 and 1.0) and the Rayleigh number (from 10^4 to 10^6) as well. By investigating five types of nanoparticles, Elif found that heat transfer rate is always an increasing function of both the nanoparticles volume fraction and the Rayleigh number. Additionally, he pointed that the nanoparticles type, the heat source length as well as the cavity inclination angle are important factors affecting the flow and temperature fields.

Oztop et al. [13] studied the effects of non-isothermal boundary conditions on natural convection in enclosures filled with (TiO_2 or Al_2O_3)-water nanofluid. The right

[a] Corresponding author: aeknad@yahoo.fr

Nomenclature

C_p	Specific heat at constant pressure (J.kg^{-1}.K^{-1})
g	Gravitational acceleration (m.s^{-2})
h	Heater' distance from the bottom wall (m)
H	Cavity height (m)
k_f	Fluid thermal conductivity (W.m^{-1}.K^{-1})
Nu	Nusselt number
$p*$	Pressure (Pa)
P	Dimensionless pressure
Pr	Prandtl number = $C_p\mu_f/k_f$
Ra	Rayleigh number = $g\beta\rho_f^2\Delta T H^3 C_p/\mu_f k_f$
T	Dimensional temperature (K)
u	Dimensional velocity component in x direction (m.s^{-1})
U	Horizontal dimensionless velocity component
v	Dimensional velocity component in y direction (m.s^{-1})
V	Vertical dimensionless velocity component
w	Heater' width (m)
x	Horizontal coordinate (m)
X	Dimensionless horizontal coordinate
y	Vertical coordinate (m)
Y	Dimensionless vertical coordinate
Greek letters	
α	Inclination angle of the cavity
α_f	Fluid thermal diffusivity (m^2.s^{-1})
β	Thermal expansion coefficient (K^{-1})
θ	Dimensionless temperature
μ_f	Fluid viscosity (kg.m^{-1}.s^{-1})
ρ_f	Fluid density (kg.m^{-3})
φ	Nanoparticles volume fraction
Ψ	Stream function
Subscript	
avg	Average
c	Cold
h	Hot
nf	Nanofluid
s	Solid particles

wall was maintained at a uniform temperature lower than the left one, which is characterized by a sinusoidal distribution. The results presented as streamlines, isotherms and Nusselt numbers for various values of Rayleigh number (10^3 to 10^5), nanoparticles volume fraction (0% to 10%), and inclination angle (0° to 90°) confirmed that under sinusoidal boundary conditions, the added nanoparticles change completely the fluid flow and the temperature distribution.

As well, the convection problem inside nanofluid filled cavities of both side walls with non-uniform heating was inspected by Arani et al. [14]. Effects of an increase in shear force when the buoyancy force is kept constant, and effects of an increase in buoyancy force for a constant shear force on the heat transfer characteristics were mainly investigated.

Regarding the effect of Brownian motion, Ghasemi and Aminossadati [15] studied the laminar steady-state natural convection into a partially heated right-angle triangular cavity filled by a CuO-water nanofluid. The CuO nanoparticles were assumed to be spherical with a radius of 10 nm. Under this condition, they proved that the Brownian motion plays a crucial role in modifying the thermal conductivity and viscosity of the nanofluid. This study and many others [16–18] validate that this effect must be only taken into account when the nanoparticles size is below 40 nm. Above this size, it can be neglected.

A few years later, the effect of magnetic field on the heat transfer through a nanofluid filled enclosure was taken into consideration, as illustrated in the paper of Aminossadati [19]. The convection phenomenon into a right-triangular cavity filled with a CuO-water nanofluid was concerned for different positions of two heat sources (which located at the bottom wall), the solid volume fraction, as well for a wide range of the Rayleigh and Hartmann numbers. The author proved that the magnetic field and the addition of nanoparticles may play an opposing role on the main heat transfer rate.

Even though there have been such studies conducted on natural convection in nanofluid filled enclosures under many configurations and boundary conditions, relatively few studies were documented in the case of cavities containing blocs [20,21]. As such, the present paper concerns the examination of laminar steady-state natural convection within a cold isosceles triangular enclosure filled with a TiO_2-water nanofluid, including a square heater at a distance $h = 0.25H$ from it base.

The main purpose of this investigation is to reveal the effect of a set of parameters such the Rayleigh number, the solid volume fraction and the inclination angle of the triangular enclosure on the heat transfer rate; to come up with general correlations which may predict the mean heat transfer into such configurations. Noted that the Brownian motion is not taken into consideration in our study since the TiO_2 nanoparticles size is assumed to be greater than 45 nm.

2 Problem's statement and mathematical formulation

The problem under investigation consists of a laminar, two dimensional natural heat transfer convection into a cold tilted isosceles triangular enclosure; having a square heater which located at a fixed distance from it bottom wall (noted as h). The physical problem as well as its boundary conditions is shown in Figure 1. The cavity area is filled with a TiO_2-water nanofluid, such as the water and TiO_2 nanoparticles are in thermal equilibrium. The computational results are obtained for a wide range of Rayleigh number ($10^4 \leq Ra \leq 10^6$) and nanoparticles volume fraction ($0\% \leq \varphi \leq 10\%$), when the enclosure inclination angle is taken between 0° and 180°. The thermo-physical properties of the base fluid and the spherical TiO_2 nanoparticles are given in Table 1. Constant thermo-physical properties are considered for the nanofluid whilst the density variation in the buoyancy forces is determined using the Boussinesq approximation [22].

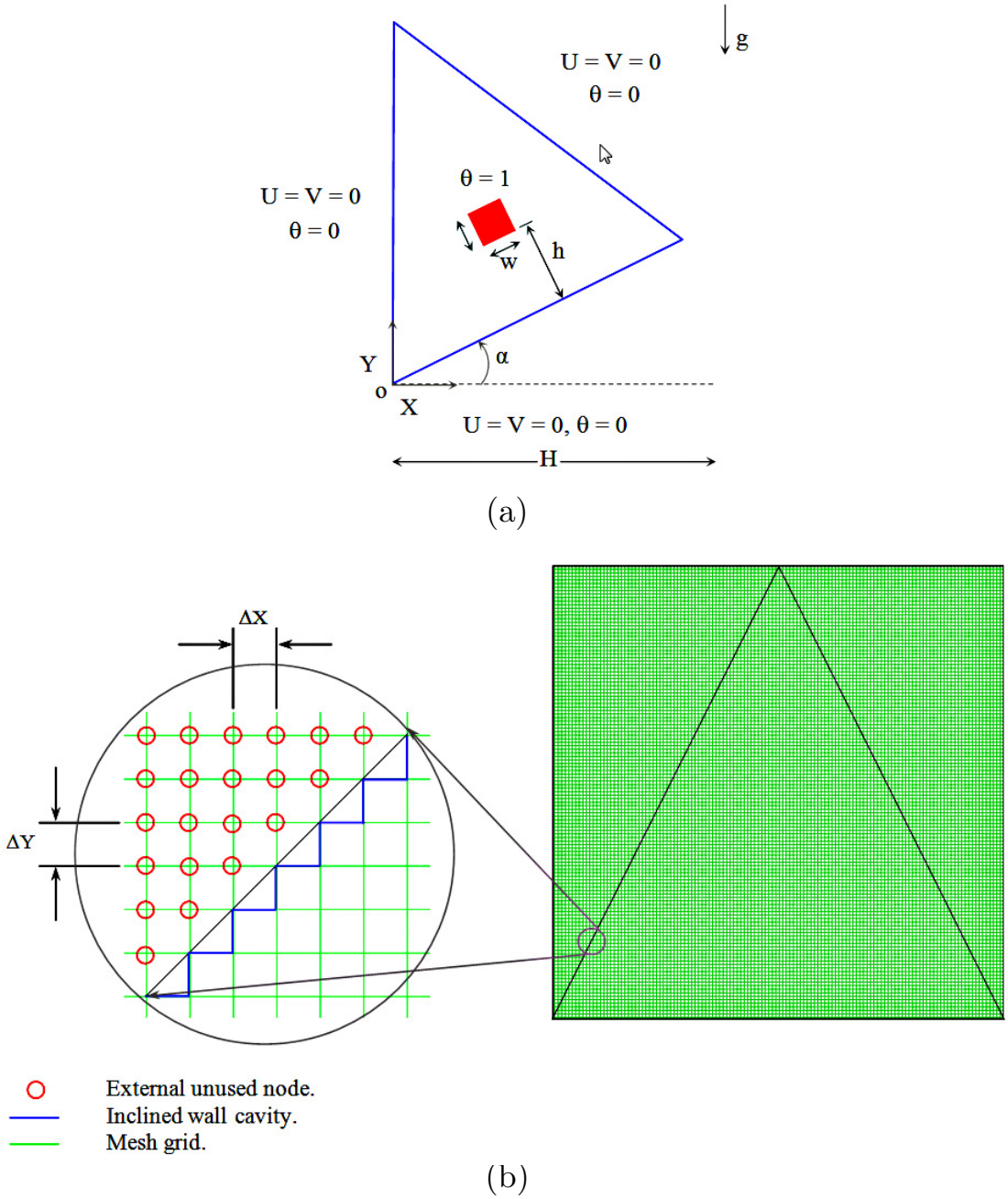

Fig. 1. Schematic of the physical problem with its boundary conditions (a) and grid arrangement (b).

Table 1. Thermo-physical properties of the base fluid and Ti_{O2} nanoparticles, $T = 25$ °C [27].

Thermo-physical properties	Base fluid (water)	TiO_2
C_p (J.kg^{-1}.K^{-1})	4179	686.2
ρ (kg.m^{-3})	997.1	4250
k (W m^{-1}.K^{-1})	0.613	8.9538
β (K) 10^{-5}	21	0.9

The density, ρ_{nf}, the heat capacity, $(\rho\, C_p)_{nf}$, the thermal expansion coefficient, $(\rho\beta)_{nf}$, and the thermal diffusivity of the nanofluid, α_{nf}, are defined, respectively, as follows [23]:

$$\rho_{nf} = (1-\varphi)\rho_f + \varphi\rho_s \quad (1)$$

$$(\rho C_p)_{nf} = (1-\varphi)(\rho C_p)_f + \varphi(\rho C_p)_s \quad (2)$$

$$(\rho\beta)_{nf} = (1-\varphi)(\rho\beta)_f + \varphi(\rho\beta)_s \quad (3)$$

$$\alpha_{nf} = \frac{k_{nf}}{(\rho C_p)_{nf}} \quad (4)$$

The effective viscosity, μ_{nf}, and the thermal conductivity, k_{nf}, of the nanofluid are obtained from the following respective relations proposed by He et al. [24] based on

their experimental results:

$$\mu_{\rm nf} = \mu_{\rm f}\left(199.21\varphi^2 + 4.62\varphi + 1.0\right) \quad (5)$$

$$k_{\rm nf} = k_{\rm f}\left(125.62\varphi^2 + 4.82\varphi + 1.0\right) \quad (6)$$

In a steady state, the dimensionless continuity, momentum (in both the horizontal and vertical directions) and the energy equations can be written as follows:

$$\frac{\partial U}{\partial X} + \frac{\partial V}{\partial Y} = 0 \quad (7)$$

$$U\frac{\partial U}{\partial X} + V\frac{\partial U}{\partial Y} = -\frac{\partial P}{\partial X} + \frac{\mu_{\rm nf}}{\rho_{\rm nf}\alpha_{\rm f}}\left[\frac{\partial^2 U}{\partial X^2} + \frac{\partial^2 U}{\partial Y^2}\right] + \sin(\alpha) \quad (8)$$

$$U\frac{\partial V}{\partial X} + V\frac{\partial V}{\partial Y} = -\frac{\partial P}{\partial Y} + \frac{\mu_{\rm nf}}{\rho_{\rm nf}\alpha_{\rm f}}\left[\frac{\partial^2 V}{\partial X^2} + \frac{\partial^2 V}{\partial Y^2}\right] + \frac{(\rho\beta)_{\rm nf}}{\rho_{\rm nf}\beta_{\rm f}} RaPr\theta + \cos(\alpha) \quad (9)$$

$$U\frac{\partial \theta}{\partial X} + V\frac{\partial \theta}{\partial Y} = \frac{\alpha_{\rm nf}}{\alpha_f}\left[\frac{\partial^2 \theta}{\partial X^2} + \frac{\partial^2 \theta}{\partial Y^2}\right] \quad (10)$$

The following dimensionless variables were introduced as:

$$X = \frac{x}{H}, Y = \frac{y}{H}, U = \frac{u\,H}{\alpha_f}, V = \frac{v\,H}{\alpha_{\rm f}}, P = \frac{p\,H^2}{\rho_{\rm nf}\,\alpha_{\rm f}^2},$$
$$\theta = \frac{T - T_{\rm c}}{T_{\rm h} - T_{\rm c}} \quad (11)$$

The Nusselt number based on the height (or the width) of the heater (w) is evaluated from the following relation:

$$Nu = \frac{h_{\rm nf} w}{k_{\rm f}} \quad (12)$$

The heat transfer coefficient for the nanofluid $h_{\rm nf}$ is obtained from the expression:

$$h_{\rm nf} = \frac{q}{T_{\rm h} - T_{\rm c}} \quad (13)$$

The heat flux on the sides of the heater per unit area q can be written as:

$$q = -k_{\rm nf}\frac{(T_{\rm h} - T_{\rm c})}{w}\left.\frac{\partial \theta}{\partial n}\right|_{\rm heater\ \ surface} \quad (14)$$

Substituting Equations (13) and (14) into Equation (12) yields to the following relation for the Nusselt number:

$$Nu = -\left(\frac{k_{\rm nf}}{k_{\rm f}}\right)\left.\frac{\partial \theta}{\partial n}\right|_{\rm heater\ surface} \quad (15)$$

where n is the normal coordinate to the heater surface.

It is to note that the average Nusselt number of the heater ($Nu_{\rm avg}$) is calculated by integrating the local Nusselt number over all four surfaces of the heater and then, divided by the perimeter of the later ($4w$).

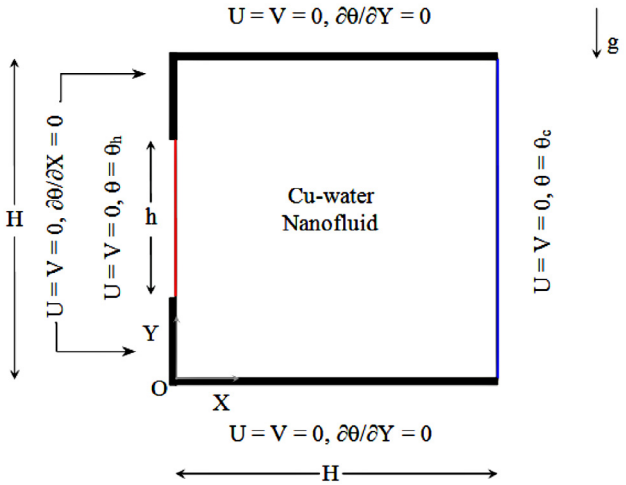

Fig. 2. Domain and boundary conditions for the buoyancy-driven heat transfer in a square cavity with a partially-heated wall filled with Cu-water nanofluid [26].

3 Numerical procedure and validation

The governing equations are discretized in space using the finite volume method. The resulting algebraic equations with its associated boundary conditions are solved using the line by line method. As the momentum equation is formulated in terms of the primitive variables (U, V and P), the iterative procedure includes a pressure correction calculation algorithm, namely SIMPLER [25], to solve the pressure-velocity coupling. Compared to other velocity-pressure coupling approaches, such SIMPLE and SIMPLEC, the SIMPLER approach is proved to be faster (about 30 to 50% fewer iterations).

The convergence criterion for the temperature, the pressure, and the velocity as well is given as:

$$\frac{\sum_{j=1}^{m}\sum_{i=1}^{n}\left|\varphi_{i,j}^{k+1} - \varphi_{i,j}^{k}\right|}{\sum_{j=1}^{m}\sum_{i=1}^{n}\left|\varphi_{i,j}^{k+1}\right|} \leq 10^{-6} \quad (16)$$

where m and n are the numbers of grid points in X- and Y-directions, respectively, φ is any of the computed field variables and k is the iteration number.

The performance of the using code via the natural convection of nanofluids into a confined space is accomplished by comparing predictions with other numerical results and experimental data, and by verifying the grid independence of the present results.

First, the present results are consistent with previous computations, namely those of Oztop and Abu-Nada [26], which deals with natural convection of Cu-water nanofluid into a partially heated square enclosure (see for instance Fig. 2). By taking into account the same hypotheses, Table 2 demonstrates a comparison of the mean Nusselt number computed with various values of the Rayleigh number (Ra) and the nanoparticles' volume fraction ($\varphi_{\rm Cu}$), respectively. As we can see, the present

Table 2. Average Nusselt number of the heat source, comparison with Oztop and Abu-Nada [26] for the partially heated square cavity filled with Cu-water nanofluid.

Ra	φ	Oztop and Abu-nada [26]	Present Work
10^3	0.00	1.004	1.005
	0.05	1.122	1.128
	0.10	1.251	1.248
	0.15	1.423	1.419
	0.20	1.627	1.621
10^4	0.00	2.010	2.032
	0.05	2.122	2.105
	0.10	2.203	2.199
	0.15	2.283	2.291
	0.20	2.363	2.382
10^5	0.00	3.983	3.992
	0.05	4.271	4.256
	0.10	4.440	4.389
	0.15	4.662	4.680
	0.20	4.875	4.861

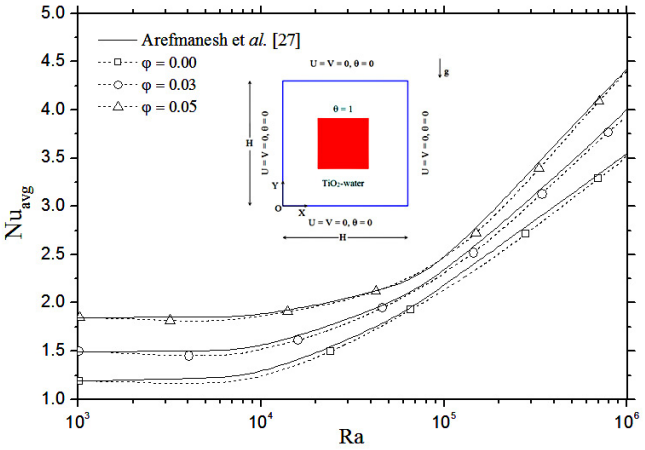

Fig. 3. Average Nusselt number evolution with Ra and φ, comparison with Arefmanesh et al. [27].

results and those of Oztop and Abu-Nada are in excellent agreement with a maximum discrepancy of about 1.8%.

To check the numerical code validity with a partitioned case, those obtained by Arefmanesh et al. [27] for a cold enclosure with a centred heater have been selected. Figure 3 illustrates the mean Nusselt number evolution with both Ra and φ_{TiO2}. Once again, the numerical predictions, obtained with a regular mesh grid of 100^2, show a great agreement with those of Arefmanesh et al.

Via the experimental data, the code boundary conditions have been adapted to those of Krane and Jessee [28] which deals with natural convection of Air into a square enclosure. Figure 4 displays the non-dimensional temperature profile at the vertical mid-plane of the enclosure and that, for a Rayleigh number equals 10^5. Regarding the latter, the numerical results exhibit a great quantitative concordance with the experimental ones, what support the use of our code via the convection phenomenon.

To ascertain the numerical code validity with triangular structures, those obtained by Varol et al. [29] have

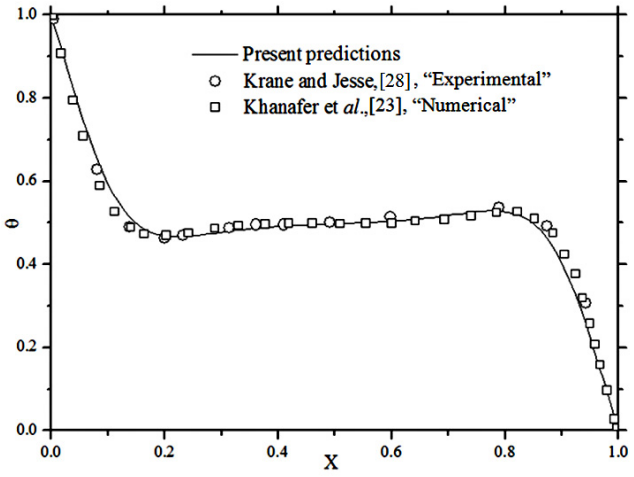

Fig. 4. Temperature distribution at the vertical mid-section of the enclosure. ($Ra = 10^5$, $Pr = 0.7$).

been taken into consideration. As reported in papers of Asan and Namli [30] and Lei et al. [31], the corner point velocity values were updated as the mean of two adjacent wall node velocity values. These boundary conditions were used to update related values on all boundaries of the triangle as the steady-state solutions were numerically approached. The discontinuity in temperature at the intersection of the inclined and base walls was handled by assuming the average temperature of the two walls at the corner and keeping the adjacent nodes at the respective wall temperatures. The inclined boundary was approximated staircase-like zigzag lines. Although the solution was computed on the approximated geometry, the resulting error in the solution for moderately fine grid is usually small [30–33]. Figure 5 displays the computed mean Nusselt number for various Rayleigh values, when a heat source is located in the middle of the vertical wall of the enclosure. As we can see, the present results and those of Varol et al. are fully identical with a maximum discrepancy of about 0.6%. In the light of these validations, the present numerical scheme may yield a very accurate velocity, temperature and Nusselt predictions for the considered problem.

In order to determine the prefect mesh for our predictions, a grid independence investigation is conducted for the convection phenomenon of TiO_2-water nanofluid into our configuration (already shown in Fig. 1a). Several mesh distributions ranging from 60^2 to 140^2 are tested, the mean Nusselt number of the above uniform grids is presented in Figure 6. It is observed that a 90^2 uniform grid is adequate for a grid independent solution. However, a fine structured mesh of 100^2 is used to avoid round-off error for all other calculations in this research.

4 Results and discussion

The results are generated for different pertinent dimensionless groups such the Rayleigh number

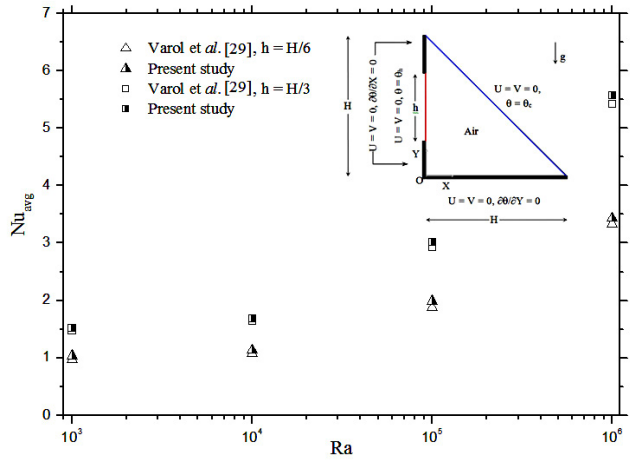

Fig. 5. The present predictions against Varol et al. [29] ones.

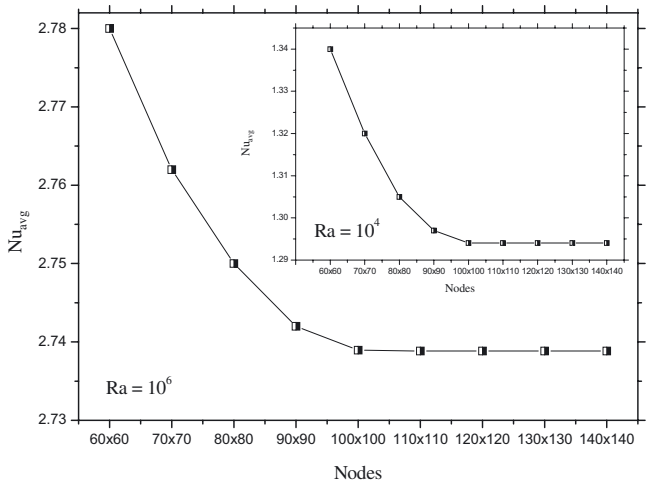

Fig. 6. Average Nusselt number for different uniform grids, $\varphi_{TiO2} = 0.04$.

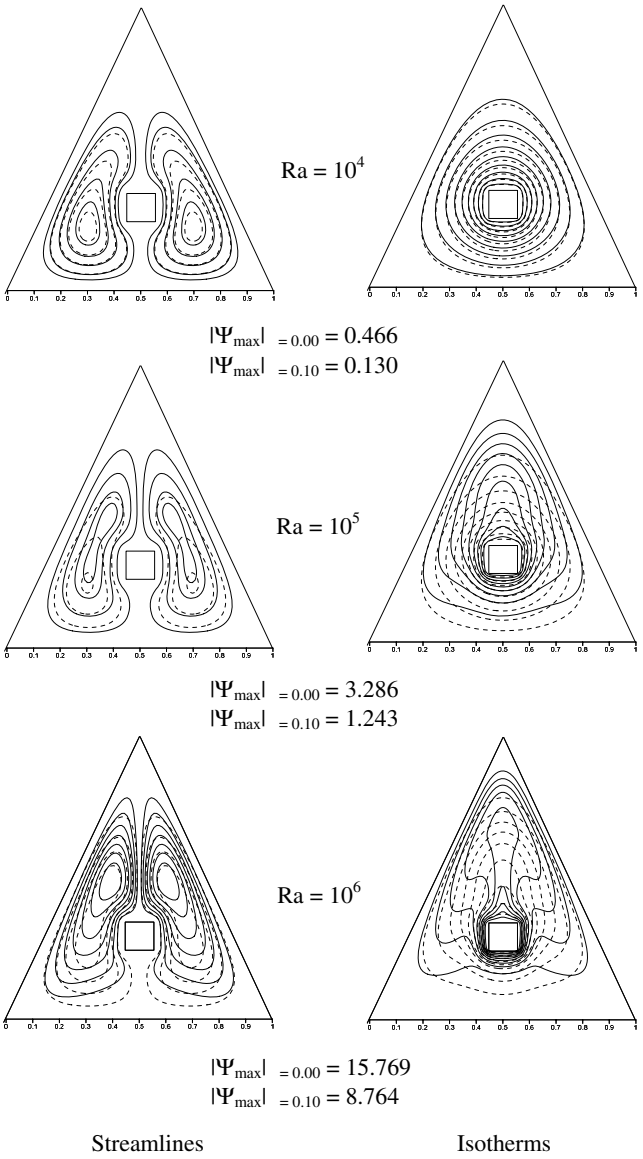

Fig. 7. Streamlines and isotherm plots for the TiO_2-water nanofluid [- - -] with $\varphi = 0.10$ and the base fluid [—].

$(10^4 \leq Ra \leq 10^6)$, the TiO_2 volume fraction $(0.0 \leq \varphi \leq 0.10)$ and the cavity inclination angle $(0° \leq \alpha \leq 180°)$. The width of the square heater as well the Prandtl number are taken equal to $0.10H$ and 6.2 respectively. The predicted (hydrodynamic and thermal) field variables are presented in terms of streamlines; isotherm plots, vertical velocity profiles and average Nusselt number.

Our investigation is carried out in two phases: in the first one, we inspect the effects of Rayleigh number and TiO_2 volume fraction on heat transfer performance into the cavity. For that, the inclination angle is kept equal to 0°. In the second, calculations are performed for a wide range of the cavity' inclination angle when the Rayleigh number and the nanoparticles volume fraction are taken as 10^6 and 0.0 (or 0.10), respectively

4.1 Impact of Rayleigh number and solid volume fraction

In this section, the inclination angle of the partitioned triangular enclosure is equal to 0°. For each value of the Rayleigh number (Ra), the predicted streamlines and isotherm plots for both values of the TiO_2 volume fraction: $\varphi = 0.10$ and $\varphi = 0.00$ (case of a pure water) are shown in Figure 7 with its related stream-functions (Ψ_{max}).

For the base-fluid case, the streamlines shows two symmetrical counter-rotating circulating cells which established in the left and the right sides of the heater. By increasing the Rayleigh number, these latter become more packed adjacent to the cold isosceles walls what makes the absolute value of the stream-function more important. When $Ra = 10^6$, the convection mechanism becomes more pronounced and consequently, the eyes of the counter-rotating eddies move upwards, indicating more densely packed streamlines at the top portion of the triangular enclosure.

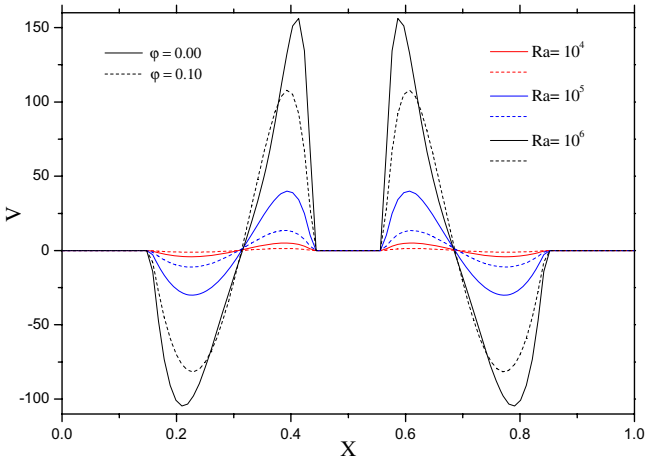

Fig. 8. Vertical velocity profiles at $Y = 0.30$ for both TiO_2-water nanofluid and pure water, according to different values of the Rayleigh number.

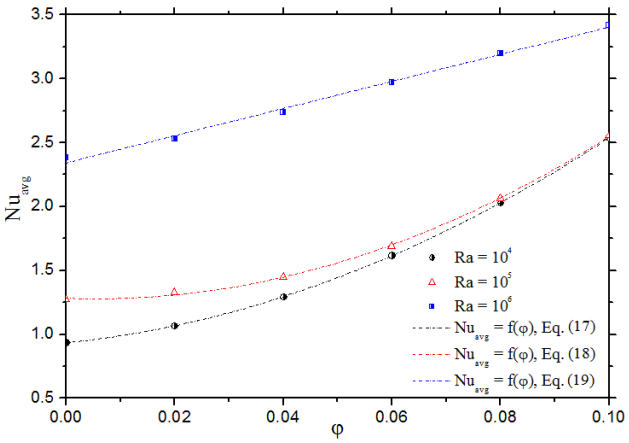

Fig. 9. Variation of the mean Nusselt number according to the nanoparticles volume fraction for various values of the Rayleigh number.

In the case of TiO_2-water nanofluid, (with $\varphi = 0.10$), the circulating cells seem weaker compared to that one of the base fluid. This phenomenon is related the fluid viscosity which becomes important with the presence of the nanoparticles.

According to Figure 7, and for a Rayleigh number of about 10^4, the isotherms are uniformly distributed, demonstrating a dominated-conduction heat transfer regime. As the Rayleigh number increases the natural convection effect becomes dominant. Therefore, thin thermal boundary layers are formed around the heater surfaces as well as along the isosceles walls indicating then, a large temperature gradient along these surfaces. It is to note that for $\varphi = 0.10$ the natural convection becomes weaker due to the TiO_2-water viscosity.

The examination of the magnitude of the vertical velocity component, along the horizontal plane at $Y = 0.30H$, for various values of Rayleigh number confirms the results previously obtained from analysing the streamlines. As displayed in Figure 8, the increase of the vertical velocity component with the Rayleigh number indicates stronger buoyant flows within the cavity. Therefore, the heat transfer mechanism is expected to be due to convection at high Rayleigh number when the conduction governs the heat transfer at low Rayleigh number. However, due to the fluid viscosity enhancement at $\varphi = 0.10$, the TiO_2-water nanofluid is associated with a lower absolute magnitude of the velocity compared to that of the pure water.

Figure 9 illustrates the mean Nusselt number (Nu_{avg}) calculated along the sides of the heat source, with respect to the volume fraction of the nanoparticles, at various values of the Rayleigh number. The mean Nusselt number is found to be an increasing function of the Rayleigh number as the heat transfer regime becomes convection dominated, and raise with the increase TiO_2 volume fraction due to the improvement of the nanofluid' thermal conductivity. Summarizing the numerical results, predictive correlations related the mean Nusselt number to the nanoparticles volume fraction, at a fixed Rayleigh number, are proposed as follows:

$$Nu_{\text{avg, } Ra=10^4} = A_1\phi^2 + A_2\,\phi + A_3 \quad (17)$$

$$Nu_{\text{avg, } Ra=10^5} = B_1\phi^2 + B_2\,\phi + B_3 \quad (18)$$

$$Nu_{\text{avg, } Ra=10^6} = C_1\phi + C_2 \quad (19)$$

where coefficients of each equation are listed in Tables 3a–3c, respectively, as well as the R^2 values to indicate the goodness of the curve-fit shown in Figure 8. These correlations are found to predict our numerical results within $\pm 0.4\%$.

4.2 Impact of the cavity inclination angle

In this section, the Rayleigh number is kept equal to 10^6 whereas the inclination angle of the cavity ranges from 0° to 180°. The main circulation cells as well as the isotherm plots are illustrated in Figure 10 and that, for two different nanoparticles volume fractions such as 0.00 and 0.10, respectively.

As we can see, the streamlines of $\alpha > 0°$ show two asymmetrical counter-rotating eddies formed inside the cavity when it is not the case for $\alpha = 180$. Additionally, the stream-function values of the investigated angles, presented in Table 4, confirm the strong rotation of the left circulating cell compared to the right one. Noted that the increase in the inclination angle leads to the increase of the weakest cell (located at the right side of the heater), to be identical to the left one what explain the symmetrical counter-rotating eddies when is equal to 180°. The isotherms for each inclination angle are adjusted according to the presented streamlines. The clustering of the isotherms towards the heater reveals a high temperature gradient and the development of thin boundary layers near its surfaces. Once again, it can be observed that the increase of the solid volume fraction decreases the natural convection phenomenon and that, because of the fluid viscosity enhancement.

Table 3. Values of curve-fit constants of (a) Equation (17), (b) Equation (18) and (c) Equation (19).

(a)	A_1	A_2	A_3	R^2 for Equation (17)
	117.2506	4.3252	0.9336	0.9999
(b)	B_1	B_2	B_3	R^2 for Equation (18)
	142.3657	–1.5739	1.2826	0.9990
(c)	C_1	C_2	R^2 for Equation (19)	
	10.6130	2.3426	0.9950	

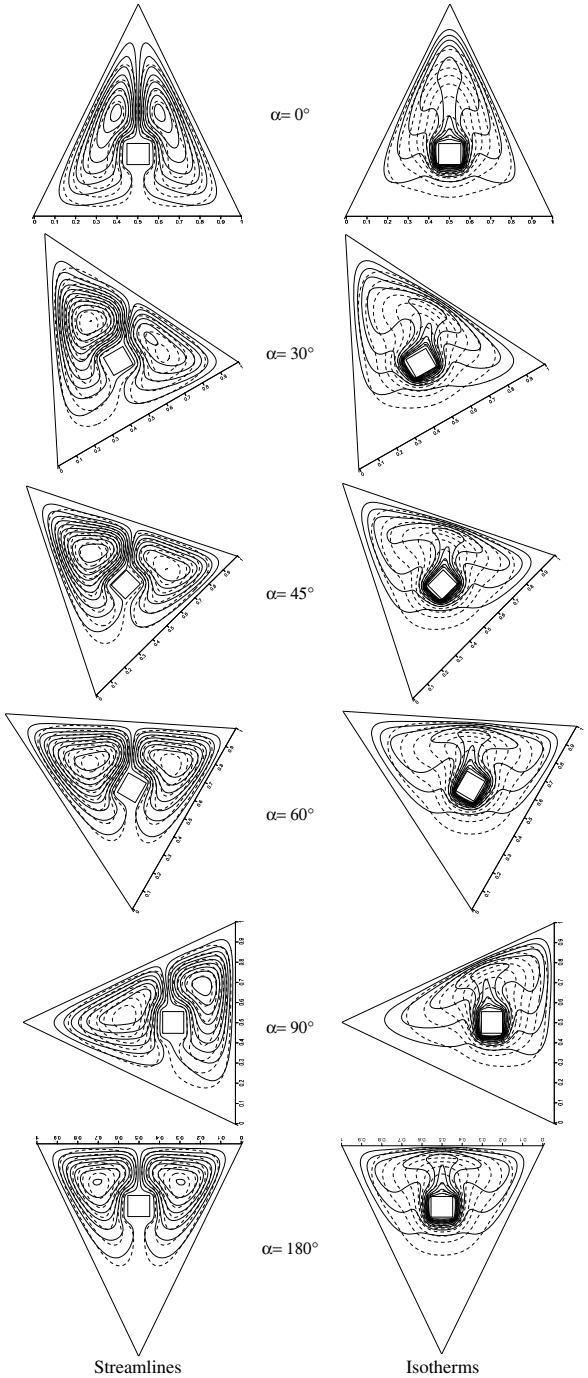

Fig. 10. Streamlines and the isotherms for Ti_{O2}-water nanofluid [- - -] with $\varphi = 0.10$ and base fluid [—], at different inclination angle.

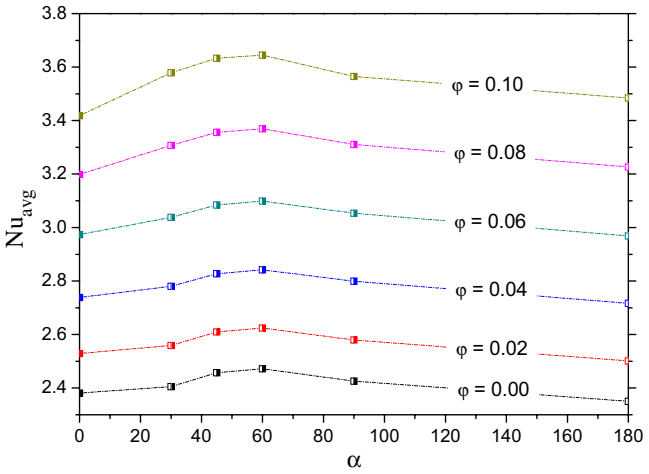

Fig. 11. Variation of the Mean Nusselt number according to the inclination angle for different values of the solid volume fraction, $Ra = 10^6$.

Table 4. Stream function of Ti_{O2}-water nanoparticles at $\varphi = 0.00$ and $\varphi = 0.10$ for various values of α.

α	Ψ_{max}		Ψ_{min}	
	$\varphi = 0.00$	$\varphi = 0.10$	$\varphi = 0.00$	$\varphi = 0.10$
0°	15.769	8.764	–15.769	–8.764
30°	20.999	16.530	–11.287	–9.569
45°	20.238	16.855	–12.640	–11.018
60°	17.833	15.905	–14.975	–12.372
90°	12.711	12.462	–18.136	–12.874
180°	15.101	12.588	–15.101	–12.588

Figure 11 shows the impact of the inclination angle on the mean Nusselt number and that, for various values of the nanoparticles' volume fraction. Unlike the positive effect of the volume fraction, the effect of the inclination angle on the heat transfer enhancement proves to be insignificant, as the maximum improvement (found with $\alpha = 60°$) is quietly over 6% compared to the non-tilted enclosure.

5 Conclusion

Natural convection heat transfer of TiO_2-water nanofluid within a cold isosceles triangular enclosure, having a square heater has been investigated numerically. The study focuses on optimal conditions leading to better heat transfer. Thus, the impacts of the Rayleigh number, the nanoparticles volume fraction as well the cavity

inclination angle on the hydrodynamic and thermal characteristics of such fluid were analyzed. The present results may summarise as follows:

- In the case of $\alpha = 0°$, the heat transfer is an increasing function of both: the Rayleigh number and the nanoparticles volume fraction.
- Useful correlations predicting the heat transfer as a function of the nanoparticles volume fraction can be proposed for each value of the Rayleigh number, which predict the numerical results within $\pm 0.4\%$.
- The increase of the inclination angle of the cavity has no significant effect on heat transfer as the maximum enhancement is quietly over 6% compared to the case of a nontilted cavity ($\alpha = 0°$). Then, the inclination of the triangular cavity is not desired to improve the heat transfer.

References

[1] S.U.S. Choi, Enhancing thermal conductivity of fluids with nanoparticles, ASME Fluids Eng. Division 231 (1995) 99–105

[2] X. Wang, X. Xu, S.U.S. Choi, Thermal Conductivity of Nanoparticle-Fluid Mixture, J. Thermophys. Heat Transfer 13 (1999) 474–480

[3] R.Y Jou, S.C. Tzeng, Numerical research of nature convective heat transfer enhancement filled with nanofluids in rectangular enclosures, Int. Commun. Heat Mass Transfer 33 (2006) 727–736

[4] A.K. Santra, S. Sen, N. Chakraborty, Study of heat transfer augmentation in a differentially heated square cavity using copper-water nanofluid, Int. J. Thermal Sci. 47 (2008) 1113–1122

[5] B. Ghasemi, S.M. Aminossadati, Natural convection heat transfer in an inclined enclosure filled with a water-CuO nanofluid, Numer. Heat Transfer A 55 (2009) 807–823

[6] E.B. Ogut, Heat transfer of water-based nanofluids with natural convection in a inclined square enclosure, J. Thermal Sci. Technol. 30 (2010) 23–33

[7] K. Kahveci, Buoyancy driven heat transfer of nanofluids in a tilted enclosure, J. Heat Transfer 132 (2010) 01–12

[8] S.M. Aminossadati, B. Ghasemi, Enhanced natural convection in an isosceles triangular enclosure filled With a nanofluid, Comput. Math. Appl. 61 (2011) 1739–1753

[9] G.A. Holtzman, R.W. Hill, K.S. Ball, Laminar natural convection in isosceles triangular enclosures heated from below and symmetrically cooled from above, J. Heat Transfer 122 (2000) 485–491

[10] E.F. Kent, Numerical analysis of laminar natural convection in isosceles triangular enclosures, Proc. Instit. Mech. Eng. Part C, J. Mech. Eng. Sci. 223-5 (2009) 57–69

[11] E.F. Kent, Numerical analysis of laminar natural convection in isosceles triangular enclosures for cold base and hot inclined walls, Mech. Res. Commun. 36 (2009) 497–508

[12] B.O. Elif, Natural convection of water-based nanofluids in an inclined enclosure with a heat source, Int. J. Thermal Sci. 48 (2009) 2063–2073

[13] H.F. Oztop, E. Abu-Nada, Y. Varol, K. Al-Salem, Computational analysis of non-isothermal temperature distribution on natural convection in nanofluid filled enclosures, Superlattices Microstruct. 49 (2011) 453–467

[14] A. Arani, S. Mazrouei, M. Mahmoodi, A. Ardeshiri, M. Aliakbari, Numerical study of mixed convection flow in a lid-driven cavity with sinusoidal heating on side walls using nanofluid, Superlattices Microstruct. 51 (2012) 893–911

[15] B. Ghasemi, S.M. Aminossadati, Brownian motion of nanoparticles in a triangular enclosure with natural convection, Int. J. Thermal Sci. 49 (2010) 931–940

[16] S.P. Jang, S.U.S. Choi, Role of Brownian motion in the enhanced thermal conductivity of nanofluid, Appl. Phys. Lett. 84 (2004) 4316–4318

[17] D. Wen, Y. Ding, Experimental investigation into convective heat transfer of nanofluids at the entrance region under laminar flow conditions, Int. J. Heat Mass Transfer 47 (2004) 5181–5188

[18] W.S. Heris, N.M. Esfahany, Gh.S. Etemad, Experimental investigation of convective heat transfer of Al_2O_3/water Nanofluid in circular tube, Int. J. Heat Fluid Flow 28 (2007) 203–210

[19] S.M. Aminossadati, Hydromagnetic natural cooling of a triangular heat source in a triangular cavity with water-CuO nanofluid, Int. Commun. Heat Mass Transfer 43 (2013) 22–29

[20] A. Mezrhab, H. Bouali, H. Amaoui, M. Bouzidi, Computation of combined natural-convection and radiation heat-transfer in a cavity having a square body at its center, Appl. Energy 83 (2006) 1004–1023

[21] M. Mahmoodi, S.M. Sebdani, Natural Convection in a Square Cavity Containing a Nanofluid and an Adiabatic Square Block at the Center, Superlattices Microstruct. 52 (2012) 261–275

[22] A. Bejan, Convection heat transfer, John Wiley & Sons, Inc., Hoboken, New jersey, USA, 2004

[23] K. Khanafer, K. Vafai, M. Lightstone, Buoyancy-driven heat transfer enhancement in a two-dimensional enclosure utilizing nanofluid, Int. J. Heat Mass Transfer 46 (2003) 3639–3653

[24] Y. He, Y. Men, Y. Zhao, H. Lu, Y. Ding, Numerical investigation into the convective heat transfer of TiO_2 nanofluids flowing through a straight tube under the laminar flow conditions, Appl. Therm. Eng. 29 (2009) 1965–1972

[25] S.V. Patankar, Numerical Heat transfer and fluid flow, Hemisphere Publishing Corporating, Taylor and Francis Group, New York, 1980

[26] H.F. Oztop, E. Abu-Nada, Numerical study of natural convection in partially heated rectangular enclosures filled with nanofluids, Int. J. Heat Fluid Flow 29 (2008) 1326–1336

[27] A. Arefmanesh, M. Amini, M. Mahmoodi, M. Najafi, Buoyancy-driven heat transfer analysis in two-square duct annuli filled with a nanofluid, Eur. J. Mech. B/Fluids 33 (2012) 95–104

[28] R.J. Krane, J. Jessee, Some detailed field measurements for a natural convection flow in a vertical square enclosure, In: 1st ASME-JSME Ther. Eng. Conf., 1983, Vol. 1, pp. 323–329

[29] Y. Varol, A. Koca, H.F. Oztop, Natural convection in a triangle enclosure with flush mounted heater on the wall, Int. Commun. Heat Mass Transfer 33 (2006) 951–958

[30] H. Asan, L. Namli, Laminar natural convection in a pitched roof of triangular cross-section: summer day boundary conditions, Energy and Buildings 33 (2000) 69–73

[31] C. Lei, S.W. Armfield, J.C. Patterson, Unsteady natural convection in a water-filled isosceles triangular enclosure heated from below, Int. J. Heat Mass Transfer 51 (2008) 2637–2650

[32] E.H. Ridouane, A. Campo, M. Mc Garry, Numerical computation of buoyant airflows confined to attic spaces under opposing hot and cold wall conditions, Int. J. Thermal Sci. 44 (2005) 944–952

[33] D.G. Briggs, D.N. Jones, Two-dimensional periodic natural convection in an enclosure of aspect ratio one, J. Heat Transfer 107 (1985) 850–854